Low-temperature localized motion of hydrogen and electronic structure transition in hexagonal-close-packed scandium

L. R. Lichty, J-W. Han, R. Ibanez-Meier,* D. R. Torgeson, and R. G. Barnes†
Ames Laboratory, and Department of Physics, Iowa State University, Ames, Iowa 50011

E. F. W. Seymour‡
Ames Laboratory, Iowa State University, Ames, Iowa 50011
and Department of Physics, University of New England, Armidale, NSW 2351, Australia

C. A. Sholl
Department of Physics, University of New England, Armidale, NSW 2351, Australia
(Received 17 June 1988)

We report nuclear magnetic resonance (NMR) measurements of the proton (^{1}H) spin-lattice relaxation rate (R_1) in the hexagonal-close-packed (hcp) solid solution (α) phase of the Sc-H system over the temperature range 10–300 K in which hydrogen pairs are known to form. At low temperatures (10–120 K), fast localized motion of hydrogen between closely spaced tetrahedral interstitial sites in the lattice gives rise to a peak in the relaxation rate. Both the temperature and frequency dependences of the relaxation rate peak exhibit characteristics typical of amorphous and disordered systems, suggesting the formation of hydrogen pairs with little long-range order results effectively in a "proton glass" within the metal lattice. The measurements reveal an electronic structure transition near 170 K where the unpaired electron spin density at the proton sites decreases with increasing temperature.

I. INTRODUCTION

The unusual ability of the rare-earth metals Sc, Y, Lu, etc., to retain substantial concentrations of hydrogen (as much as 30%) in solid solution to very low temperatures without precipitating an ordered hydride phase has lately been the object of considerable investigative effort. Neutron diffraction measurements[1] on α-ScD$_{0.33}$ have shown hydrogen occupies only the tetrahedral interstitial sites in the hcp Sc lattice. As shown in Figs. 1(a) and 1(b), the tetrahedral sites occur in close pairs (A and B; C and D) along the c axis. Neutron diffraction has also shown in the similar Lu-H and Y-H solid solution phases[2,3] hydrogen tends to order in pairs of tetrahedral sites oriented along the c axis of the hcp lattice and separated by an intervening metal atom [B and C in Figs. 1(a) and 1(b)]. The concentration of such pairs increases with decreasing temperature.[3] Moreover, according to the model proposed[3] to explain the most recent neutron scattering data for Y-H solid solutions, pairs tend to congregate along c-axis chains, and near 170 K arrange themselves along the c axis of a chain with a regular spacing. This latter degree of ordering is thought to be related to an electronic structure change. The pairing phenomenon was first proposed[4] as the cause of the resistivity anomaly found in all of these systems at temperatures in the vicinity of 170 K. A recent neutron spectroscopic study[5] has revealed the hydrogen-bonding potential in α-YH$_x$ is both strongly anisotropic and anharmonic along the c axis of the lattice.

In a previous NMR study,[6] evidence for the originally proposed[4] "close pairing" of hydrogens in adjacent tetrahedral sites [separation $\simeq 1.35$ Å, shown by A and B (and also C and D) in Figs. 1(a) and 1(b)] was sought in the α-YH$_x$ system. Pairs of protons so closely spaced would yield a characteristic "Pake doublet" NMR spectrum readily distinguishable in α-YH$_x$ because of the negligible line broadening due to the neighboring metal nuclei (the nuclear moment of ^{89}Y equals about 0.05 of the proton). No indication whatever of such doublet structure was found, consistent with the more recent neutron results[2,3] described above in which the paired proton-proton spacing is about 5.0 Å. In the work reported here, we have utilized the dynamic, rather than static, response of the proton spins and have concentrated on the α-ScH$_x$ system in which the substantial ^{45}Sc magnetic moment makes the dominant contribution to the motionally induced spin-lattice relaxation of the protons.

II. EXPERIMENT

The solid-solution (α) phase ScH$_x$ samples were prepared from high- purity Ames Laboratory (Materials Preparation Center) scandium metal having a total rare-earth impurity content of <5 parts per million (ppm) and and iron content of 13 ppm determined by mass-spectrographic analysis. Preparation involved reacting the bulk metal with hydrogen gas to obtain the dihydride ScH$_2$ which was then crushed (in an inert atmosphere) to fine powder suitable for the NMR measurements. Sufficient hydrogen was then extracted under vacuum at high temperature to bring the composition into the solid-solution range, the final composition being deter-

mined by high-temperature vacuum extraction. Samples were sealed in quartz tubes under low inert gas pressure for the NMR.

Measurements of the proton spin-lattice relaxation rate (R_1) were made at resonance frequencies of 24, 40, 62 or 65, and 90 MHz (0.564, 0.939, 1.46, 1.53, and 2.11 T, respectively). The phase-coherent pulsed NMR spectrometer and associated instrumentation have been described elsewhere.[7] These measurements were made using a saturation comb of four or five 90° pulses followed τ seconds later by another 90° pulse which sampled the recovered magnetization, observing the free-induction decay (FID) signal (i.e., 90°-comb-τ-90°-FID). The magnetization recovery signals were exponential at all temperatures, resonance frequencies, and hydrogen concentrations.

The low-temperature measurements were made in a continuous-flow helium cryostat incorporating a home-built metal Dewar probe with a "Helitran LTD-3-110" transfer tube, cold finger, and control unit. The metal Dewar was used in order to avoid unwanted proton resonance signals from hydrogen in the original Helitran Pyrex Dewar. In the home-built probe the NMR coil is located within the Dewar chamber and contains only the sample tube so the filling factor is significantly improved in comparison to the commercial unit in which the coil encloses the Dewar. The tuning circuit for the rf coil is located outside the Dewar at room temperature. Coarse temperature control is achieved by regulating the flow of He gas leaving the Dewar. A chromel–(Au+0.07 at. % Fe) thermocouple mounted on the Helitran cold-finger controls a heater to provide a temperature stability of ±0.2 K. The sample temperature is monitored by a second Chromel–(Au-Fe) thermocouple in contact with the sample but removed during data-accumulation runs to reduce electrical noise.

III. RESULTS

A. Overview

As examples of the observed temperature dependence of R_1, we show in Fig. 2 the ^{1}H measurements in α-ScH$_{0.27}$ over the temperature range 10–280 K at 62 MHz and over the temperature range 6–140 K at 24 MHz. Two features are strikingly evident. First, a peak in R_1
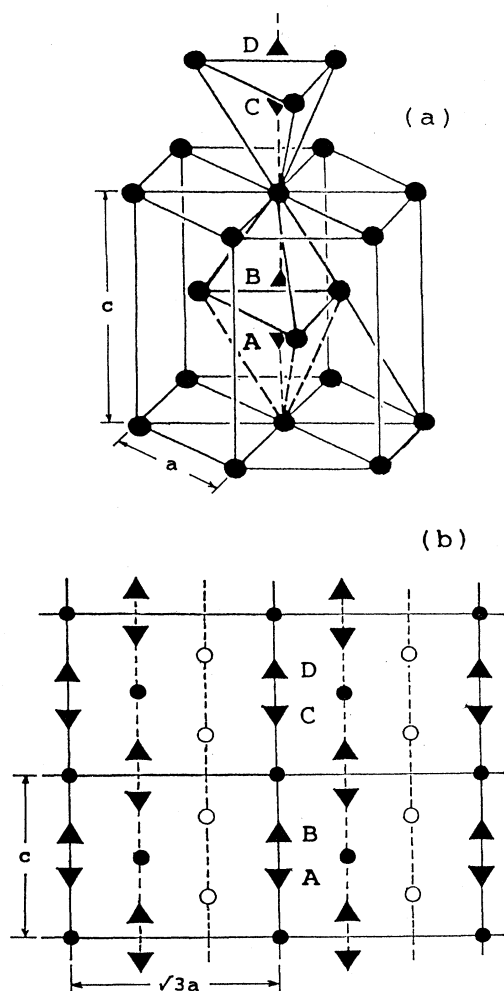
FIG. 1. (a) Hexagonal close-packed metal lattice (solid circles) showing the location of the tetrahedral interstitial sites (solid triangles). Sites A and B (and also C and D) form a close pair separated by $\sim 0.25c$. (b) Cross section in the cb plane of the hcp lattice showing the location of both tetrahedral (solid triangles) and octahedral (open circles) sites. As in (a), sites A and B form a close pair.
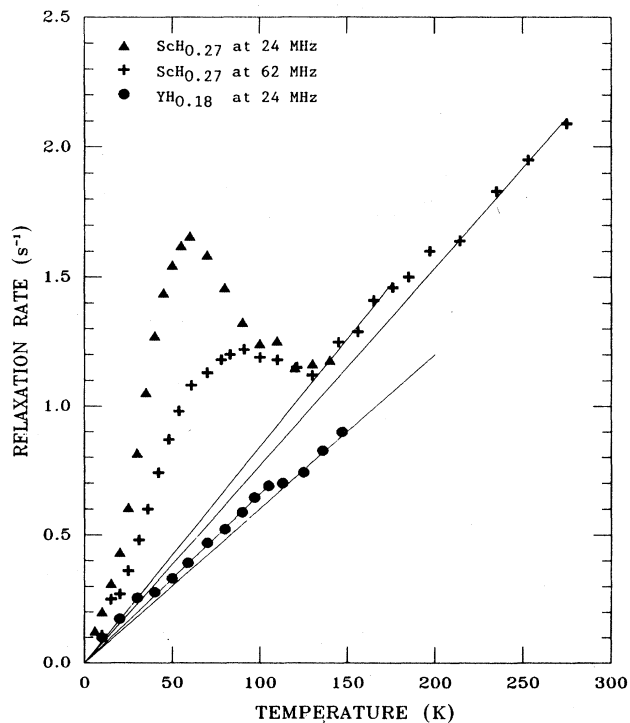
FIG. 2. Temperature dependence of the proton R_1 in α-ScH$_{0.27}$ measured at 24 and 62 MHz. The upper two solid lines represent the Korringa product T/R_{1e} for temperatures above and below ~ 170 K for α-ScH$_{0.27}$. Also shown is R_1 vs T in α-YH$_{0.18}$ measured at 24 MHz.

appears centered at ~ 60 K at 24 MHz and at ~ 80 K at 62 MHz. This peak is superimposed on the underlying conduction-electron contribution (R_{1e}) indicated by the straight dashed lines representing the constancy of the Korringa product, $T_{1e}T = T/R_{1e}$, expected to hold for this contribution to the total rate R_1.[8] A second feature appears in the range 180–200 K. Since this feature is independent of frequency and also appears in $YH_{0.18}$ with comparable magnitude (see below), it is not of motional origin, and we interpret it as a decrease in T/R_{1e}. Measurements on samples with $x = 0.057$ and 0.11 reveal similar behavior of R_1 over the same temperature range.

Figure 2 also shows the temperature dependence of the proton R_1 in $YH_{0.18}$ at 24 MHz. The much weaker relaxation peak at ~ 30 K in this case reflects directly the much weaker ^{89}Y-^1H magnetic dipolar interaction in comparison to the ^{45}Sc-^1H interaction. Indeed, the ^{89}Y-^1H interaction is so weak the majority of the peak is due to the ^1H-^1H dipolar interaction. The change in Korringa product is also evident, although at a somewhat lower temperature.

We associate the change in Korringa product with a change in the product of the d-band contribution to the electronic density of states, $N_d(E_F)$, and the hyperfine field H_{CP}^d arising from core polarization by the d electrons of filled states derived from hydrogen $1s$ orbitals.[9] The low-temperature peak in R_1 we associate with rapid hydrogen motion within pairs of closely spaced tetrahedral sites such as A, B in Fig. 1, any more extensive translational motion being essentially frozen out at these temperatures. Indications that this inference is correct follow from plots of the "localized motion" R_1 peak itself $(R_{1L} = R_1 - R_{1e})$, which display qualitatively the expected dependence on the proton resonance (Zeeman) frequency ω_H at low and high temperatures. This is shown for the $x = 0.27$ data at all four resonance frequencies in the conventional form, $\log_{10}R_{1L}$ versus $1000/T$, in Fig. 3(a) and for the $x = 0.11$ data in Fig. 3(b). (i) On the high-temperature side of the maximum rate, R_{1L} is independent of ω_H, whereas it is ω_H dependent on the low-temperature side. (ii) The maximum rate $R_{1L,max}$ increases with decreasing ω_H, as expected. (iii) The temperature T_{max} where the maximum rate $R_{1L,max}$ occurs increases with increasing frequency. In addition, it is seen the maximum rate is relatively insensitive to the hydrogen concentration.

An additional especially striking feature of the data is the relative weakness of the maximum relaxation rate $R_{1L,max}$. This is seen in Fig. 4 which shows the temperature dependence of R_1 from 6 to 640 K at 40 MHz for the $x = 0.27$ sample. Compared to the strength $R_{1d,max}$, where R_{1d} is defined by $R_{1d} = R_1 - R_{1e}$ for the temperature range $T > 300$ K, the relaxation peak occurs at high temperatures (~ 500 K) due to the full three-dimensional diffusive motion of the hydrogen measured in the same samples,[10] we have $R_{1L,max} \simeq 0.015R_{1d,max}$. Moreover, $R_{1d,max}$ itself is only $\sim 75\%$ of the calculated full dipolar interaction at the proton sites.[10] The latter observation shows unambiguously $\sim 25\%$ of the full dipolar interaction has been averaged away by very fast localized hydro-

gen motion and is no longer effective for relaxation at high temperatures. On this basis alone, we would expect $R_{1L,max} \simeq 0.33R_{1d,max}$. The much weaker value of $R_{1L,max}$ observed shows additional factors must contribute to reducing this value. Several candidates for this role are (1) a distribution of hopping times associated with different potential barriers at different hydrogen sites, (2) localized motion between potential wells of unequal depth, and (3) the fraction of hydrogens responsible for the relaxation.

B. Electronic structure change

As remarked above, the change in Korringa product observed in the vicinity of 180 K (Fig. 2) reflects a change in the product of H_{CP}^d and $N_d(E_F)$. In general in transition metals and their hydrides, the s-band contribution to the density of states $N_s(E_F)$ is negligible in comparison to $N_d(E_F)$, even though the s electron hyperfine field H_s is usually greater than H_{CP}^d, the d-band contribution dominates the electronic contribution to the spin-lattice relaxation. Furthermore, as discussed by Bowman *et al.*,[9] in transition-metal–hydrogen systems there is both experi-
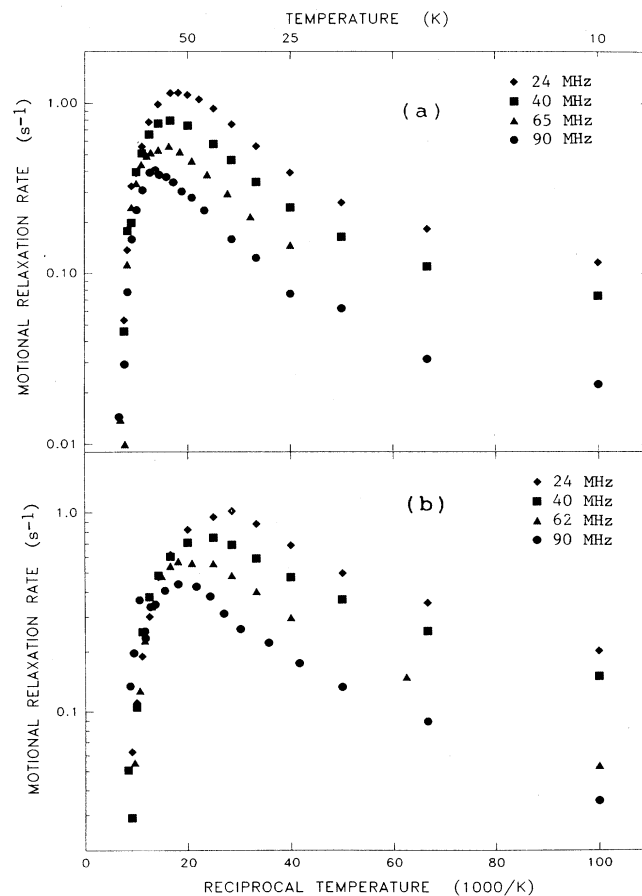
FIG. 3. (a) Dependence of the motional contribution $R_{1L} = R_1 - R_{1e}$, on reciprocal temperature $1000/T$ for $x = 0.27$, determined at resonance frequencies of 24, 40, 62, and 90 MHz. (b) The same for the $x = 0.11$ sample.
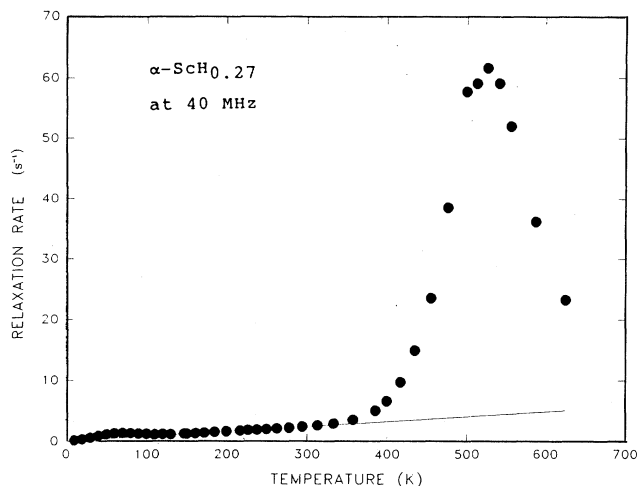
FIG. 4. Temperature dependence of the measured proton R_1 over the entire range 6–625 K for $x = 0.27$ at 40 MHz. The dashed line shows the Korringa product $T_{1e}T = 123$ s K.

mental and theoretical evidence the d-electron orbital contribution is unimportant. The result is $(T_{1e}T)^{-1/2} \propto [H_{CP}^d N_d(E_F)]$. Here, $H_{CP}^d \propto \langle |\Phi_{CP}(0)|^2 \rangle$ with

$$|\Phi_{CP}(0)|^2 \propto \sum_n a_{1s}(0) a_{ns}(0) \, ,$$

where the a's are the amplitudes of the 1s and ns wave functions at the origin. Thus, the change in Korringa product observed may reflect changes in both the density of states and the electronic wave functions themselves. For the α-ScH$_x$ data shown in Fig. 2, typical for the $x = 0.27$ sample, the increase in $T_{1e}T$ from 117 ± 2 s K to 124 ± 2 s K with increasing temperature at the transition corresponds to a decrease of $3.0\% \pm 0.5\%$ in the product $|\Phi_{CP}(0)|^2 N_d(E_F)$. For the $x = 0.11$ sample, the decrease is $4.2\% \pm 0.8\%$, and for the $x = 0.05$ sample, it is $4.7\% \pm 1.0\%$ where the greater uncertainties reflect the poorer signal-to-noise ratio quality of the resonance in the lower hydrogen concentration samples. Thus for all compositions, the decrease in $|\Phi_{CP}(0)|^2 N_d(E_F)$ at the transition is about 4%. The results for α-YH$_{0.18}$, shown in Fig. 2, are closely similar, amounting to a decrease of $3.9\% \pm 0.5\%$. If the observed changes are predominantly due to a change in charge density associated with a regular arrangement of proton pairs along the c axis, then the percentages reflect electronic charge density changes at occupied proton sites. Alternatively, the changes in $T_{1e}T$ might result primarily from changes in $N_d(E_F)$. Most probably, both factors contribute to the observed changes and are not readily separated. We do not have reliable proton Knight shift (K) data and hence cannot utilize the value of the Korringa constant $K^2 T_{1e} T$ to carry out a more detailed analysis.

C. Low-temperature behavior

If the motion responsible for the spin-lattice relaxation results from a single thermally activated process, it is well known[11] the relaxation rates in the high- and low-temperature limits are proportional to τ_d and $\omega_H^{-2} \tau_d^{-1}$, respectively, where τ_d is the mean dwell time for the motion. Hence, if $\tau_d = \tau_0 \exp(E/k_B T)$, where E is the activation energy, τ_0 the reciprocal of the attempt frequency, and k_B Boltzmann's constant, then in a graph of $\log_{10} R_1$ versus the same (apart from a negative sign) and equal to E/k_B. This is clearly not the case in Fig. 3, the slopes on the low-temperature sides of the peaks being substantially weaker than on the high-temperature side. Moreover, the low-temperature sides do not display a constant slope in this graph (i.e., plotted against $1000/T$), but rather decrease with decreasing temperature. Also evident in Fig. 3 is the fact the temperature T_{max} at which $R_{1L,max}$ occurs decreases with decreasing hydrogen content.

Since it can be shown (see Sec. IV B 2) for localized motion between two potential wells, the resulting dipolar field fluctuations decay exponentially, yielding a Lorentzian spectral density as in the Bloembergen-Purcell-Pound (BPP) model,[12] we expect $R_{1L,max} \propto \omega_H^{-1}$. As seen in Fig. 5, the slope of $\log_{10} R_{1L,max}$ versus $\log_{10} \omega_H/2\pi$ for the $x = 0.11$ sample is -0.65 rather than -1. Also shown in Fig. 5 are the data points for T fixed at 30 K for $x = 0.27$. These show the frequency dependence on the low-temperature side of the maximum rate goes as $\omega_H^{-1.2}$ rather than as ω_H^{-2} expected on the basis of Lorentzian spectral densities. Thus, both the maximum rate and the rate in the long correlation time limit of the low-temperature motion display a dependence on resonance frequency substantially weaker than expected. As is evident from Fig. 1, and confirmed by calculation (see Sec. IV B 2), the one-dimensional proton motion does not imply the dipolar interaction fluctuations are even approximately described by a one-dimensional model, so the
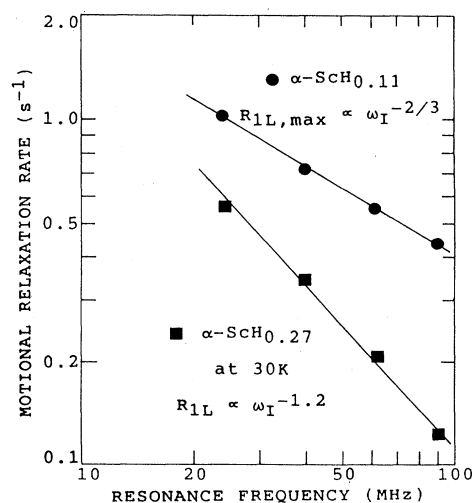
FIG. 5. Dependence of the maximum rate $R_{1L,max}$ on resonance frequency, ω_H for the $x = 0.11$ sample, showing $R_{1L,max} \propto \omega_H^{-2/3}$. Also shown is the dependence of the rate R_{1L} on ω_H at $T = 30$ K for the $x = 0.27$ sample, showing here $R_{1L} \propto \omega_H^{-1.2}$.

weak frequency dependence expected for such systems, $\omega_H^{-0.5}$ in the long correlation time limit, cannot be relevant here (see for example Ref. 13 for a treatment particularly relevant to hexagonal symmetry). In contrast, the relaxation rate at high temperatures ($T > 400$ K), R_{1d}, follows BPP behavior closely,[10] showing long-range diffusion of hydrogen in the Sc lattice is governed by a single correlation time as in simple liquids.

These several features of the R_{1L} data are closely similar to those found for nuclear spins in disordered systems. For example, the inequality of the high- and low-temperature side slopes, seen in Fig. 3, has been found for hydrogen in random alloys[14] and amorphous intermetallic compounds.[15] It is a well-known feature of the nuclear spin-lattice relaxation rate in both organic[16,17] and inorganic[18,19] glasses and in fast-ion conductors.[20] This characteristic behavior results from the presence of a distribution of correlation times, resulting from either (or both) a distribution of activation energies or of prefactors, reflecting in turn a distribution of interstitial well depths and perhaps shapes.

Finally, we note at fixed frequency ω_H the maximum motional relaxation rate $R_{1L,\max}$ is only weakly dependent on the hydrogen concentration x, the $R_{1L,\max}$ values indicating a decreasing trend with decreasing x. These values and the temperatures $T_{\max}$ at which $R_{1L,\max}$ occurs are summarized in Table I. The low hydrogen concentration in the $x = 0.057$ sample made quantitative measurements unreliable at 62 and 90 MHz.

IV. DISCUSSION

A. Electronic structure change

The recent study[3] of the temperature dependence of diffuse neutron scattering in single-crystal α-YD$_{0.17}$ suggests an order-disorder transition in deuterium arrangement occurs between 170 and 280 K. Two features of these measurements stand out. (1) The temperature dependence of the broad ridge of scattering intensity in a plane normal to the (00l) direction at $\sim\frac{4}{3}$ (the so-called "planar feature") indicates the deuterons have formed pairs on next-nearest tetrahedral sites along the c direction of the yttrium lattice and shows a rather abrupt change in slope at ~ 180 K. (2) In contrast, the fraction of paired deuterons changes relatively smoothly over this same temperature range, and moreover remains quite high (43%) even at 350 K. Correspondingly, the changes

in the proton $T_{1e}T$ product we have observed in all the samples studied [α-ScH$_x$, α-YH$_x$, and α-LuH$_x$ (Ref. 21)] also occur within narrow temperature intervals ($\Delta T \sim 20$ K). The same is true of the temperature dependence of the resistivity[4] wherein the anomalous behavior is primarily a change in the slope of $\rho(T)$ and occurs in a similar rather narrow temperature range.

In this respect then, all three sets of measurements indicate a rather abrupt change occurs at the temperature at which the neutron study shows the degree of ordering of pairs of deuterons along the c axis has essentially reached its maximum value. The $T_{1e}T$ results reported here indicate this change is accompanied by (or gives rise to) an electronic structure transition. This conclusion is not inconsistent with the ideas presented in Ref. 3, that is, the interaction driving the ordering of pairs is electronic in origin, having its basis in the structure of the Fermi surface of the group-IIIb metals in a manner similar to the interactions responsible for the spiral magnetization of dilute alloys of magnetic rare earths in yttrium, for example. As remarked above (Sec. III B), the change in $T_{1e}T$ may reflect a change in the density of states, the electronic charge density at the proton, or both. It is easy to imagine the transition involves a very small change in Fermi surface structure, for example.

B. Low-temperature motion

1. Introduction

As described in Sec. III C, the low-temperature behavior of $R_{1L} = R_1 - R_{1e}$ is typical of proton relaxation resulting from hydrogen motion. Neglecting the proton-proton contribution (which never exceeds 7% of the total in the α phase of Sc-H), the dipolar spin-lattice relaxation rate R_{1m} due to hydrogen motion of any kind may be described by an equation of the general form

$$R_{1m} = \gamma_H^2 \Delta M_2 F(\omega_H, \omega_{Sc}, \tau_c) , \qquad (1)$$

where γ_H and ω_H are the proton gyromagnetic ratio and Zeeman frequency, respectively, ω_{Sc} is the ^{45}Sc Zeeman frequency, ΔM_2 is that part of the dipolar second moment at a proton site due to all ^{45}Sc nuclear moments caused to fluctuate in time by the motion, and $F(\omega_H, \omega_{Sc}, \tau_c)$ is a spectral density function describing the dependence of the dipolar field fluctuations on ω_H, ω_{Sc}, and the correlation time τ_c for the fluctuations. In turn,

TABLE I. Resonance frequency and composition (x) dependence of the maximum motional relaxation rate $R_{1L,\max}$ and the temperature $T_{\max}$ of the maximum rate. Values of $R_{1L,\max}$ have an estimated uncertainty of $\pm 10\%$, and those of $T_{\max}$ of ± 3 K.

Resonance frequency (MHz)	$x = 0.27$		$x = 0.11$		$x = 0.057$	
	$T_{\max}$ (K)	$R_{1L,\max}$ (s^{-1})	$T_{\max}$ (K)	$R_{1L,\max}$ (s^{-1})	$T_{\max}$ (K)	$R_{1L,\max}$ (s^{-1})
24	55	1.16	35	1.02	36	0.85
40	60	0.80	40	0.72	40	0.64
62	66	0.58	47	0.65		
90	73	0.38	55	0.44		

τ_c is approximately equal to the mean dwell time for hydrogen hopping which is temperature dependent, and F is a function of T as well. R_{1m} reaches its maximum value when $\omega_H \tau_c \simeq 1$. Hopping rates, significantly slower or faster than ω_H are relatively ineffective in causing relaxation.

In α-ScH$_x$ the high-temperature (~ 500 K) R_{1d} measurements[10] show the maximum rate $R_{1d,\max}$ is only $\sim 75\%$ of the value that results from taking ΔM_2 to be the full rigid-lattice second moment M_2. This shows $\sim 25\%$ of M_2 has already been rendered ineffective by a faster hydrogen motion than that responsible for long-range diffusion and is no longer capable of promoting relaxation at high temperatures.

Quasielastic neutron scattering measurements on α-YH$_{0.2}$ at high temperatures[22] indicate hydrogen diffusion occurs via tetrahedral-octahedral-tetrahedral jump paths, and similar behavior is expected in α-ScH$_x$. The controlling step must be the tetrahedral-octahedral jump since there is no evidence hydrogen resides for any detectable time in the octahedral sites. The neutron measurements also show at high temperatures tetrahedral-tetrahedral jumps occur at a very high rate compared to tetrahedral-octahedral jumps. These results are easily compatible if the hydrogen motion consists of very fast localized tetrahedral-tetrahedral motion [between sites A and B or C and D in Figs. 1(a) and (b)] superimposed on the relatively slower tetrahedral-octahedral motion responsible for long-range diffusion. From the lattice geometry we calculate (see further below) the fast tetrahedral-tetrahedral motion averages away $\sim 25\%$ of M_2, leaving $R_{1d,\max}$ determined by the remaining 75%, thereby accounting for the high-temperature results. We then expect the fast tetrahedral-tetrahedral motion to be responsible for the motional relaxation peak at low temperatures when the tetrahedral-tetrahedral hopping rate $\tau_L^{-1}(\mathrm{TT}) \simeq \omega_H$.

The observed R_{1L} could arise predominantly from paired or unpaired hydrogens. The pairing phenomenon observed at low temperatures by neutron diffraction[2,3] indicates sites B and C must have somewhat deeper potential minima than sites A and D. Thus, the localized motion of a paired proton must surely occur between potential wells of unequal depth. This in itself causes a weakening of the maximum relaxation rate to an extent dependent on the inequality. However, the localized motion responsible for R_{1L} may be a property of only that small fraction of protons which remain unpaired at low temperatures, and this also would weaken the maximum rate. The neutron scattering measurements show 93% of the hydrogens in α-YH$_{0.17}$ are already paired at 120 K.[3] Assuming the paired hydrogens are locked in place and only the unpaired ones are free to jump rapidly between the closely spaced tetrahedral sites (and the paired hydrogens dissociate with increasing temperature before their localized tetrahedral-tetrahedral hopping rate increases to $\sim \omega_H$), the relaxation rate due to this motion results essentially entirely from the modulation of the ^{45}Sc contribution to the dipolar field at the unpaired proton sites. The consequent relaxation (or magnetiza-

tion) of these protons is transferred to other proton spins via spin diffusion for which we estimate a rate, $\tau_{HH}^{-1} \sim 5 \times 10^4$ s^{-1}, much faster than the observed R_{1L}. Thus, the proton spin system is characterized by a single spin-lattice relaxation rate R_1, as observed. (Spin diffusion is not involved in this case; R_{1L} is a result of the majority paired hydrogens. All protons individually possess the same R_{1L}.) Either of these pictures can also account for the much weaker effect seen in α-YH$_{0.18}$ (in Fig. 2) due to the extremely small ^{89}Y moment. A discussion of the third possibility referred to in Sec. III A, a distribution of potential barriers, is deferred to Sec. IV A 3 b.

To summarize, the most significant features of the low-temperature data are (a) the small value of the maximum rate $R_{1L,\max}$ compared to the maximum relaxation rate at high temperatures $R_{1d,\max}$, (b) the marked difference in the slopes of the high- and low-temperature sides of the $\log_{10}R_{1L}$ versus $1000/T$ plots (Fig. 3), (c) the weak dependence of both $R_{1L,\max}$ and R_{1L} at long correlation times on ω_H, and (d) the fact that at fixed ω_H, $R_{1L,\max}$ depends only weakly on the hydrogen context x.

2. Theoretical background

In order to derive some quantitative conclusions from the measurements and to show the latter are indeed consistent with localized motion at low temperatures, we develop an expression for the temperature dependence of the motional relaxation rate R_{1m} appropriate to the entire temperature range. We take into account both the localized nature of the low-temperature motion and the possibility this motion occurs between wells of unequal depth, as well as the long-range diffusive motion at high temperatures. The averaging of the nuclear dipolar interaction, and subsequent reduction in the effectiveness of long-range motion for spin-lattice relaxation, resulting from localized motion between potential wells A and B of unequal depth has been treated by Look and Lowe[23] and Anderson,[24] among others, for cases of hindered rotation by molecular groups. The essential feature of this approach is the dipolar relaxation rate is reduced by a factor dependent on the energy difference Δ between the potential minima.

Neglecting the proton-proton contribution to R_{1m}, the general expression [Eq. (1)] for the relaxation rate due to the proton-scandium interactions is given by[25]

$$R_{1m} = \gamma_H^2 \gamma_{Sc}^2 \hbar^2 S(S+1)[\tfrac{1}{12}J^{(0)}(\omega_H - \omega_{Sc}) + \tfrac{3}{2}J^{(1)}(\omega_H)$$
$$+ \tfrac{3}{4}J^{(2)}(\omega_H + \omega_{Sc})] , \qquad (2)$$

where γ_{Sc} and ω_{Sc} are the ^{45}Sc gyromagnetic ratio and Zeeman frequency, respectively. The $J^{(q)}(\omega)$ are the spectral density functions and are related to the correlation functions $G^{(q)}(t)$ of the fluctuating dipolar fields by

$$J^{(q)}(\omega) = 2 \operatorname{Re} \int_0^\infty G^{(q)}(t) \exp(-i\omega t) dt . \qquad (3)$$

For a polycrystalline sample, the powder average $\langle G^{(q)}(t) \rangle_{av}$ is needed,

$$\langle G^{(q)}(t)\rangle_{av}=\frac{d_q^2}{8\pi}\sum_{r_j,r_k}\frac{3\cos^2\theta_{jk}-1}{r_j^3 r_k^3}P(\mathbf{r}_j,\mathbf{r}_k,t)\ ,\quad (4)$$

where $\mathbf{r}_j$ and $\mathbf{r}_k$ are vectors from a given Sc nucleus to the two hydrogen tetrahedral sites between which the localized motion occurs, and θ_{jk} is the angle between these vectors $[j,k=A,B$ in Figs. 1(a) and 1(b)]. $P(\mathbf{r}_j,\mathbf{r}_k,t)$ is the probability a proton is at $\mathbf{r}_j$ at $t'=0$ and at $\mathbf{r}_k$ at $t'=t$. The factor $d_0^2=16\pi/5$, and $d_0^2:d_1^2:d_2^2=6:1:4$, as usual.

Applying the method and notation of Anderson[24] to the two-well system and ignoring for the moment the possibility of jumps away from the pair of sites, the contributions from various equivalent groups of Sc neighbors to $\langle G^{(0)}(t)\rangle_{av}$, for example, always take the form

$$\langle G^{(0)}(t)\rangle_{av}=(4/5c^6)\{C_1-C_2Q_A(1-Q_A)$$
$$\times[1-\exp(-W_1-W_2)t]\}\ ,\quad (5)$$

where c is the c-axis lattice parameter and C_1 and C_2 are lattice sums. It will become clear C_1 is the rigid-lattice sum and C_2 takes account of the local motion. The W's are the transition probabilities for hydrogen hopping from site A to site B $(W_1=W_{A\to B})$ and from B to A $(W_2=W_{B\to A})$, and $Q_A=W_2/(W_1+W_2)$ is the equilibrium occupation of site A. In this way we allow for the possibility the two wells may not be of equal depth due to the random proximity of other single or paired hydrogens

or to the possibility sites B and C, for instance, constitute a pair. W_1 and W_2 are given by

$$W_1=\tau_{0L}^{-1}\exp[-(H+\Delta)/k_BT]$$

and

$$W_2=\tau_{0L}^{-1}\exp[-H/k_BT]\ ,\quad (6)$$

and where $\Delta=E_A-E_B$ is the difference in energy between the bottom of the wells, H is the energy barrier between the wells measured from the larger of E_A,E_B, and τ_{0L} is the reciprocal of the attempt frequency for the low-temperature localized motion. Hence, Q_A is given by $[1+\exp(-\Delta/k_BT)]^{-1}$. We have assumed the same prefactor τ_{0L}^{-1}, although this is not necessary. We do not expect these to be very different, in any event. Equation (5) shows the localized motion leads exactly to exponentially decaying correlation functions.

To include the effect of jumps away from sites A and B at higher temperatures, it is necessary to include a further term in the rate equations for the site-occupancy probabilities. A model in which an atom in A or B at $t=0$ with probability unity exchanges between A and B as before, but has a probability governed by W_3 of jumping away altogether (and not returning), has the exact effect of multiplying the previous expressions for $G^{(q)}(t)$ by $\exp(-W_3t)$, and leads finally to a general expression for the $J^{(q)}(\omega)$:

$$J^{(q)}(\omega)=d_q^2\frac{4}{15c^6}C_1\left[\frac{W_3}{W_3^2+\omega^2}-\frac{C_2}{C_1}Q_A(1-Q_A)\frac{W_3}{W_3^2+\omega^2}+\frac{C_2}{C_1}Q_A(1-Q_A)\frac{W_1+W_2}{(W_1+W_2)^2+\omega^2}\right]\ ,\quad (7)$$

with $(W_1+W_2)\gg W_3$. This last expression can be rewritten in more conventional form by noting $W_3=\tau_d^{-1}$, where τ_d is the mean dwell time for long-range hydrogen hopping (i.e., tetrahedral-octahedral jumps), $W_1+W_2=\tau_L^{-1}$,[23] is the localized hopping rate, and $4Q_A(1-Q_A)=\mathrm{sech}^2(\Delta/2k_BT)$:[23]

$$J^{(q)}(\omega)=d_q^2\frac{1}{15c^6}\left[[4C_1-C_2\mathrm{sech}^2(\Delta/2k_BT)]\frac{\tau_d}{1+\omega^2\tau_d^2}+C_2\mathrm{sech}^2(\Delta/2k_BT)\frac{\tau_L}{1+\omega^2\tau_L^2}\right]\ .\quad (8)$$

With this expression for the $J^{(q)}(\omega)$ the relaxation rate R_{1m} of Eq. (2) can be written as $R_{1m}=R_{1L}+R_{1d}$, where the rates R_{1L} and R_{1d} due to localized and long-range motion, respectively, are given by

$$R_{1L}=\frac{\gamma_H^2M_2^{\text{H-Sc}}}{2\omega_H}\frac{C_2}{4C_1}\mathrm{sech}^2(\Delta/2k_BT)F(\omega_H,\omega_{Sc},\tau_L)\ ,\quad (9)$$

and

$$R_{1d}=\frac{\gamma_H^2M_2^{\text{H-Sc}}}{2\omega_H}\left[1-\frac{C_2}{4C_1}\mathrm{sech}^2(\Delta/2k_BT)\right]$$
$$\times F(\omega_H,\omega_{Sc},\tau_d)\ ,\quad (10)$$

with

$$F(\omega_H,\omega_{Sc},\tau)=\frac{\omega_H\tau}{1+(\omega_H-\omega_{Sc})^2\tau^2}+\frac{3\omega_H\tau}{1+\omega_H^2\tau^2}$$
$$+\frac{6\omega_H\tau}{1+(\omega_H+\omega_{Sc})^2\tau^2}\quad (11)$$

providing the explicit form of the spectral density functions. In Eqs. (9) and (10) we have also explicitly displayed the rigid-lattice second moment,

$$M_2^{\text{H-Sc}}=(4/15)\gamma_{Sc}^2\hbar^2S(S+1)C_1c^{-6}\ .\quad (12)$$

To apply these results to α-ScH$_x$ the lattice sums C_1 and C_2 need to be evaluated using Eq. (4). From Eqs. (9) and (10) it is evident C_2 is the lattice sum corresponding to that part of the second moment affected by the localized motion and, as shown in Eq. (12), C_1 is the sum for the rigid-lattice second moment. These sums are functions of the c/a ratio and of the hydrogen locations in the lattice. For $x=0.27$, for example, we use the lattice parameters $a=3.335$ Å, $c=5.293$ Å, and $c/a=1.587$.[26]

3. Application to the measurements

We can now compare the measurement results with the appropriate theoretical expressions to obtain some quantitative conclusions about the hydrogen motions.

a. Effective second moment at high temperatures. From Eq. (12), the rigid-lattice second moment $M_2 \propto C_1$ (the superscript H-Sc is omitted for brevity). At low temperatures, with the hydrogen frozen in one well and the hydrogen positions being $0.375c$ and $0.625c$, we obtain $C_1 = 1653$ (units of c^{-6}) from Eq. (4) for $x = 0.27$. When the localized motion is sufficiently fast but the bulk (long-range) motion is negligible, we have $Q_A = 0.5$, $\text{sech}^2(\Delta/2k_B T) = 1$, $\exp(-t/\tau_d) = 1$, and $\exp(-t/\tau_L) = 0$, with the result the effective second moment at high temperatures is, from Eq. (10),

$$M_2|_{\text{fast}} = M_2|_{\text{rigid}}[1 - (C_2/4C_1)] .$$

The hydrogen positions are then $0.395c$ and $0.605c$, yielding $C_2 = 1810$. Accordingly, the ratio $M_2|_{\text{fast}}/M_2|_{\text{rigid}} = 0.728$. Worth noting is the fact that this result is independent of the asymmetry Δ between the well depths. The calculated value of $M_2|_{\text{rigid}} = 12.2$ Oe^2,[10] so the calculated $M_2|_{\text{fast}} = 8.9$ Oe^2. Experimentally, the high-temperature measurements[10] found $M_2|_{\text{fast}} = 8.8$ Oe^2, in excellent agreement with the value expected from the reduction due to the fast localized motion.

b. Temperature and frequency dependence of R_{1L}. From Eq. (6) the localized hopping rate at low temperatures, $\tau_L^{-1} = W_1 + W_2$, is given by

$$\tau_L^{-1} = \tau_{0L}^{-1}[1 + \exp(-\Delta/k_B T)]\exp(-H/k_B T) , \quad (13)$$

where H is the barrier height (activation energy) for the motion. Since $\Delta < 240$ K (a rough estimate obtained by comparing $R_{1L,\text{max}}$ with Eq. (9), assuming all protons take part in the motion (see also Sec. IV B 3 c), the term $[1 + \exp(-\Delta/k_B T)] \simeq 1$, so this factor may be taken as unity. However, because of the apparent lack of correlation between the locations of hydrogen pairs situated on adjacent lines parallel to the c direction,[3] we expect H, and therefore τ_L as well, not to possess unique values but to be characterized by distributions. As already mentioned, this situation is typical for spin-lattice relaxation in many classes of disordered solids.

The calculation of R_{1L} follows from Eqs. (9) and (11), but with the spectral density of Eq. (11) "distributed" by introducing a distribution function $g(\tau)$ which is folded with the spectral density in evaluating R_{1L}. In recent applications of this procedure to hydrogen in metals,[14,15] the distribution of τ values has been attributed to a distribution of activation energies $g(H)$ taken to be a Gaussian for simplicity and for ease of visualization of the result. However, other functions have been widely applied to the analysis of motional relaxation in disordered materials. In the case of glasses[16-19] the Cole-Davidson function, and for fast-ion conductors, the Kohlrausch-Williams-Watts function (stretched exponential)[20] have been used. We consider here primarily the application of a Gaussian distribution of activation energies to the present measurements.

(i) *Gaussian distribution of activation energies.* The distribution of τ_L values [Eq. (13)] may result from either or both a distribution in H or τ_{0L} (the effect of Δ is negligible). For simplicity and on the basis of experience with

hydrogen in random alloys,[14] we neglect the small changes in τ_{0L} that may occur and attribute the distribution of τ_L to a distribution of H, namely,

$$g(H) = N \exp[-(H - H_0)^2/2\sigma^2] .$$

The calculation of R_{1L} then becomes

$$R_{1L} = \int_0^{\infty} R_{1L}(H)g(H)dH , \quad (14)$$

where $R_{1L}(H)$ is given by Eq. (9) with $\tau_L = \tau_L(H)$ from Eq. (13). In this way, we account for both the temperature and resonance frequency dependence of R_{1L} with a single set of parameters.

In applying Eq. (14) to fit $R_{1L}(\omega_H, T)$, in addition to the constants γ_H, ω_H, ω_{Sc}, the calculated value[10] of the second moment $M_2^{\text{H-Sc}}$ was used. In order to allow for the possibility the weakness of R_{1L} may result in part from the motion of only a fraction of all the hydrogen, the factor $(C_2/4C_1)\text{sech}^2(\Delta/2k_B T)$ in Eq. (9) was replaced by a parameter C representing the product of the two contributions Δ and the hydrogen fraction to the strength. The possible interpretations of this parameter are discussed further below. The fitting parameters were then C, H_0, σ, and τ_{0L}.

On this basis, least-squares fits were made to the data for each composition and frequency. As an example, the data and fit for $x = 0.27$ at 40 MHz are shown in Fig. 6. The resulting fit parameters are listed in Table II. These values indicate the 62-MHz data for $x = 0.27$ are inconsistent with the other data sets—the resulting parameter values are anomalous, presumably due to some systematic error in the measurements. A simultaneous fit to all of the data points (equally weighted) at the three frequencies (24, 40, and 90 MHz) was also made, and the result is shown by the solid curves in Fig. 7. It is clear a distribution of hopping rates can account for the asymmetry in the temperature dependence of R_{1L}. However, the substantial width of the distribution required is somewhat disconcerting. Since for a Gaussian, the half width at half height is 1.18σ, the σ values obtained from the fits (Table II) cause the distribution to have considerable
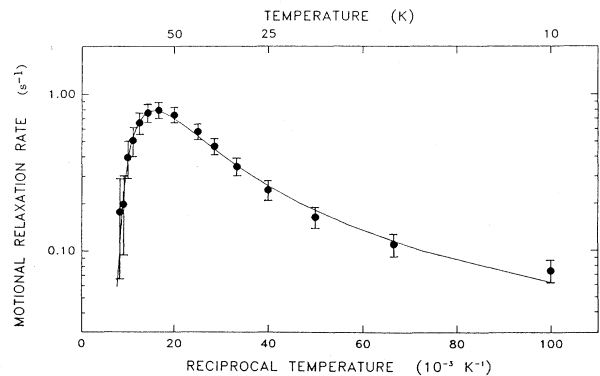
FIG. 6. Dependence of the motional relaxation rate R_{1L} on reciprocal temperature for $x = 0.27$ at 40 MHz. The solid curve is the least-squares fit of Eq. (14) to the data using a Gaussian distribution of activation energies. The resulting fit parameters are listed in Table II.

TABLE II. Least-squares-fit parameters resulting from the fit of Eq. (14) to the R_{1L} data shown in Figs. 3 and 6. The parameter $M_2 = 12.2$ Oe^2 was held fixed.

$\omega/2\pi$ (MHz)	24	40	62	90	All[a]
H_0 (meV)	57	50	82	61	52
σ (meV)	38	31	38	29	30
τ_{0L} (10^{-14} s)	0.18	2.3	0.011	1.1	2.1
C	0.054	0.048	0.067	0.046	0.045

[a] 62-MHz data excluded.

weight at zero energy.

For the $x = 0.11$ and 0.057 samples, the application of Eq. (14) with a Gaussian distribution $g(H)$ leads to anomalously short values of τ_0 and to σ values equal to or greater than H_0. For example, for $x = 0.11$ at 40 MHz we obtain $H_0 = 41$ meV, $\sigma = 42$ meV, $\tau = 2.1 \times 10^{-16}$ s, and $C = 0.075$.

(ii) *Stretched exponential distribution.* An alternative approach to representing a distribution of exponentially decaying correlation functions is to employ the so-called stretched-exponential (Kohlrausch-Williams-Watts) function[20,27,28]

$$f(t) = \exp[-(t/\tau)^\beta]$$
$$= \int \exp(-t/\tau)g(\tau)d\tau , \qquad (15)$$

where $g(\tau)$ is again a distribution function whose width is now characterized by the exponent β. Although the shape of the distribution $g(\tau)$ is not readily visualized, the exponent β is given by the ratio of the apparent activation energies on the low- and high-temperature sides of the $\log_{10}R_{1L}$ versus $1000/T$ graph, and in addition, the low-temperature frequency dependence should be given by $\omega^{(1+\beta)}$.[20,28] We can, therefore, estimate for the $x = 0.27$ sample, for example, $\beta \simeq 0.2$.
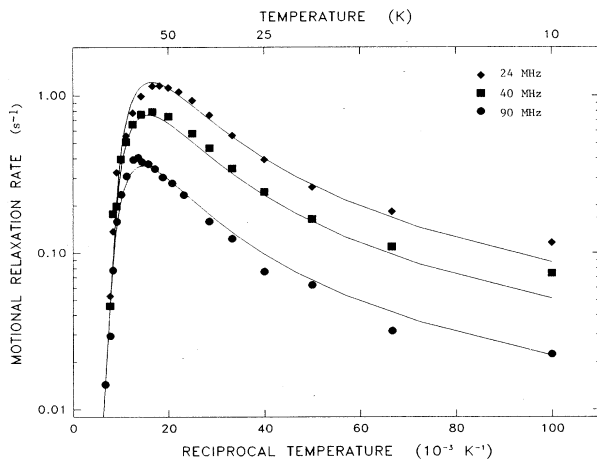
FIG. 7. Dependence of R_{1L} on reciprocal temperature for $x = 0.27$ at 24, 40, and 90 MHz (data on Fig. 3). The solid curves are the least-squares fit of Eq. (14) to the data using a Gaussian distribution of activation energies. The resulting parameters are listed in Table II.

c. Relative strength of the low-temperature rate R_{1L}. In comparing the strength of the relaxation rate R_{1L} at low temperatures $R_{1L,\mathrm{max}}$ to the long-range diffusive motion at high temperatures $R_{1d,\mathrm{max}}$, it is essential to recognize the distribution of hopping times employed in fitting Eq. (14) to the data reduces $R_{1L,\mathrm{max}}$ in comparison to what would be obtained if the distribution width $\sigma = 0$. An estimate of this effect was obtained on the basis of the Gaussian distribution of H by synthesizing the behavior of R_{1L} as $\sigma \rightarrow 0$, using the other fit parameters from Table II. The distribution widths σ found from the fits (Table II) reduce $R_{1L,\mathrm{max}}$ by a factor of 0.2. The remaining reduction of $R_{1L,\mathrm{max}}$ must then be ascribed to the parameter C used in the fitting process (Sec. IV B 3 b), which includes the effects of both the difference in potential well depths Δ and the fraction of hydrogen in motion. Experimentally (Sec. III A), $R_{1L,\mathrm{max}}/R_{1d,\mathrm{max}} \simeq 0.015$ for the $x = 0.27$ composition. Therefore, we have $0.2C \simeq 0.015$ or $C \simeq 0.075$.

If the potential wells between which the localized motion occurs are of equal depth, as might be suspected for unpaired hydrogens, then $\Delta = 0$, and the parameter C represents solely the fraction of hydrogen involved in the localized motion at low temperatures. As already noted (Sec. IV B 1), the neutron scattering measurements[3] show 93% of the hydrogens in α-YH$_{0.17}$ are paired at 120 K and may be near or at the limit of the extent of pairing. Thus, 7% would remain unpaired, in excellent agreement with the value of C.

On the other hand, it is conceivable the great majority of paired hydrogens participate in the localized motion, and the reduction in strength of R_{1L} results entirely from the effect of the difference in well depths Δ. We then have

$$(C_2/4C_1)\mathrm{sech}^2(\Delta/2k_B T) \simeq 0.075 .$$

With $C_2/4C_1 = 0.272$, we have $\mathrm{sech}^2(\Delta/2k_B T) \simeq 0.28$, from which we obtain $\Delta \simeq 22$ meV (240 K), taking $T = T_{\mathrm{max}} = 60$ K for this composition and frequency. In fact, the situation is surely somewhat more complex, since it is likely a distribution in the values of Δ also occurs for the same reasons we expect a distribution in H. However, attempting to accomodate all of these possibilities in the fitting process does not lead to unambiguous results.

Finally, we remark in regard to the trend of the $R_{1L,\mathrm{max}}$ values (Table I) to increase with increasing hydrogen concentration. This trend might result from changes in the parameter Δ characterizing the difference in well depths, or from a change in the distribution σ, for example. It might also reflect a change in the fraction of unpaired hydrogen with changing concentration. A third possibility is this trend results from the proton-proton contribution to the dipolar second moment which has been neglected in the calculations. The ^{45}Sc contribution $M_2^{\mathrm{H\text{-}Sc}}$ to the rigid-lattice second moment, which does not depend explicitly on hydrogen concentration, decreases with increasing hydrogen concentration due to the accompanying increase in lattice parameter c.[26] On the other hand, the proton contribution $M_2^{\mathrm{H\text{-}H}}$ increases be-

cause it is directly proportional to the hydrogen concentration.

The good fit to the data with $C \sim 7\%$ tends to support the correctness of this interpretation the motional peak is due to unpaired proton motion. The inequivalence of sites within a close pair would then have to do with strains and other proton-neighbor arrangements, and the parameters governing the local motion would be subject to a spread of values. It is conceivable, however, there could be some contribution from paired protons. Here there is clearly a built-in inequivalence associated with pairing.

V. SUMMARY AND CONCLUSIONS

Measurements of the temperature (10–300 K) and frequency (24–90 MHz) dependence of the proton spin-lattice relaxation rate at three concentrations of hydrogen in solid solution in hcp scandium are reported. These measurements reveal unambiguously the occurrence of an electronic structure change at ~ 170 K where the product of the charge density at the proton sites and the electronic density of states decreases by roughly 4% with increasing temperature. At low temperatures (10–120 K), fast localized motion of hydrogen between closely spaced tetrahedral sites in the lattice gives rise to a relaxation peak. Although the data are consistent with residual, unpaired hydrogen as the origin of this motional peak, an alternative interpretation in terms of asymmetrical localized motion of paired hydrogen atoms cannot be ruled out. This identification is confirmed by the magnitude of the relaxation rate reflecting long-range hydrogen motion at high temperatures. Both the temperature and frequency dependence of the low-temperature relaxation rate peak exhibit characteristics typical of amorphous and disordered systems, thus suggesting the formation of hydrogen pairs with little long-range order results effectively in a "proton glass" within the metal lattice.

*Present address: Department of Physics, Rice University, Houston, Texas.

†Present address: National Science Foundation, Division of Materials Research, Room 408, 1800 G Street N.W., Washington, D.C. 20550.

‡Present address: Department of Physics, University of Warwick, Coventry CV4 7AL, U.K.

[1]C. K. Saw, B. J. Beaudry, and C. Stassis, Phys. Rev. B 27, 7013 (1983).

[2]O. Blaschko, G. Krexner, J. N. Daou, and P. Vajda, Phys. Rev. Lett. 55, 2876 (1985).

[3]M. W. McKergow, D. K. Ross, J. E. Bonnet, I. S. Anderson, and O. Schaerpf, J. Phys. C 20, 1909 (1987); J. E. Bonnet, D. K. Ross, D. A. Faux, and I. S. Anderson, J. Less-Common Metals 129, 287 (1987).

[4]J. E. Bonnet, C. Juckum, and A. Lucasson, J. Phys. F 12, 699 (1982).

[5]I. S. Anderson, J. J. Rush, T. Udovic, and J. M. Rowe, Phys. Rev. Lett. 57, 2822 (1986).

[6]L. Lichty, R. J. Schoenberger, D. R. Torgeson, and R. G. Barnes, J. Less-Common Metals 129, 31 (1987).

[7]T-T. Phua, B. J. Beaudry, D. T. Peterson, D. R. Torgeson, R. G. Barnes, M. Belhoul, G. A. Styles, and E. F. W. Seymour, Phys. Rev. B 28, 6227 (1983).

[8]J. Korringa, Physica (Utrecht) 16, 601 (1950).

[9]R. C. Bowman, Jr., E. L. Venturini, B. D. Craft, A. Attalla, and D. B. Sullenger, Phys. Rev. B 27, 1474 (1983).

[10]J-W. Han, C-T. Chang, D. R. Torgeson, E. F. W. Seymour, and R. G. Barnes, Phys. Rev. B 36, 615 (1987).

[11]R. M. Cotts, in Hydrogen in Metals I, Basic Properties, edited by G. Alefeld and J. Volkl (Springer, Berlin, 1978).

[12]N. Bloembergen, E. M. Purcell, and R. V. Pound, Phys. Rev.

73, 679 (1948) (referred to as BPP).

[13]C. A. Sholl, J. Phys. C 14, 447 (1981).

[14]L. Lichty, J. Shinar, R. G. Barnes, D. R. Torgeson, and D. T. Peterson, Phys. Rev. Lett. 55, 2895 (1985).

[15]J. T. Markert, E. J. Cotts, and R. M. Cotts, Phys. Rev. B 37, 6446 (1988).

[16]T. M. Connor, Trans. Faraday Soc. 60, 1574 (1964).

[17]W. Mueller-Warmuth and W. Otte, J. Chem. Phys. 72, 1749 (1980).

[18]E. Goebel, W. Mueller-Warmuth, H. Olyschlaeger, and H. Dutz, J. Magn. Reson. 36, 371 (1979).

[19]G. Balzer-Joellenbeck, O. Kanert, J. Steinert, and H. Jain, Solid State Commun. 65, 303 (1988).

[20]J. L. Bjorkstam, J. Listerud, and M. Villa, Solid State Ionics 18&19, 117 (1986).

[21]D. R. Torgeson, J-W. Han, C-T. Chang, L. Lichty, R. G. Barnes, E. F. W. Seymour, and G. W. West, International Symposium on Metal-Hydrogen Systems, Stuttgart, Federal Republic of Germany, 1988, Proceedings of the Conference [Z. Phys. Chem. (to be published)].

[22]I. S. Anderson, A. Heidemann, J. E. Bonnet, D. K. Ross, S. K. P. Wilson, and M. W. McKergow, J. Less-Common Met. 101, 405 (1985).

[23]D. C. Look and I. J. Lowe, J. Chem. Phys. 44, 3437 (1966).

[24]J. E. Anderson, J. Magn. Reson. 11, 398 (1973).

[25]A. Abragam, The Principles of Nuclear Magnetism (Clarendon, Oxford, 1961).

[26]B. J. Beaudry (private communication).

[27]H. Huber, M. Mali, J. Roos, and D. Brinkman, Phys. Rev. B 37, 1441 (1987).

[28]W. T. Sobol, I. G. Cameron, M. M. Pintar, and R. Blinc, Phys. Rev. B 35, 7299 (1987).